Research on numerical analysis method of sensible heat flux from building external surfaces in an existing old residential district

Kan Chen*
Tongji Architectural Design (Group) Co., Ltd., Shanghai, China

ABSTRACT

The renovation of existing residential district is being promoted in major cities across China, including Shanghai. Therefore, it is important to improve the thermal environment in surrounding areas of buildings. Sensible heat flux from building external surfaces is a key factor influences the thermal environment. In order to clarify sensible heat flux, it is significant to understand the distributions of convective heat transfer coefficient (CHTC) and surface temperature. This study used 3D CAD-based thermal-environment simulator which can calculate building surface temperatures by heat balance simulation. By coupling the heat balance simulation with computational fluid dynamics (CFD), the study examines the relationships between wall-adjacent wind velocity and CHTC to derive a prediction equation which can be apply to the prediction of CHTC for High Reynolds number k-ε model (the High-Re model). Finally, the study examines the prediction accuracy of the prediction equation by comparison with the Jürges equation. The results show that the prediction equation for the High-Re model is appropriate for predicting the sensible heat flux from the building external surfaces under the forced convection field.

Keywords: CHTC, sensible heat flux, CFD, numerical analysis, heat transfer, prediction equation

1. INTRODUCTION

With the acceleration of aging and the establishment of carbon neutrality goals in China, the renovation of existing residential district is being promoted in major cities including Shanghai. Improving the thermal environment around the buildings in these existing residential districts is one of the methods suitable for aging and reduce building carbon emissions. The sensible heat flux from building external surfaces is a primary cause of atmospheric warming around the buildings, creating uncomfortable thermal environment and causing heat-island effects. Therefore, it has become essential to quantitatively study the sensible heat flux from the external surfaces of buildings.

The sensible heat flux can be expressed by the following equation:

$$q_c = \mathrm{CHTC}\ (T_s - T_{ref}) \tag{1}$$

where q_c is sensible heat flux, CHTC is convective heat transfer coefficient, T_s is surface temperature, and T_{ref} is reference temperature outside the temperature boundary layer.

As shown in Equation (1), CHTC and the surface temperature are essential factors for estimating the sensible heat flux. To identify elements of the surface-temperature distribution, previous study1 developed a three-dimensional (3D) computer-aided design (CAD)-based thermal-environment simulator which can calculate building surface temperatures based on the weather condition, the detailed geometries of the buildings, and the constituent materials (Figure 1). While detailed geometries affect the sensible heat flux from building external surfaces2, there have been few research studies quantitatively in confirming the sensible heat flux distribution.

This study aims to clarify the properties of CHTC and sensible heat flux distribution on building external surfaces by numerical simulation.

2. RESEARCH METHOD

2.1 CHTC identification

There are three main methods for identifying CHTC: field measurements, wind-tunnel experiments, numerical simulation.

* soryuw@foxmail.com

Third International Conference on Computer Science and Communication Technology (ICCSCT 2022)
edited by Yingfa Lu, Changbo Cheng, Proc. of SPIE Vol. 12506, 125062D
 · 0277-786X · doi: 10.1117/12.2662526

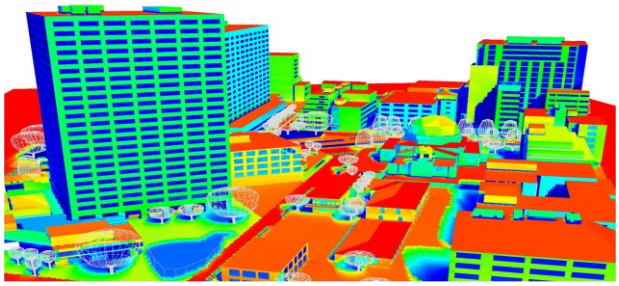

Figure 1. Surface-temperature distribution of urban blocks calculated by the 3D CAD-based thermal environment simulator.

Field measurements were performed in earlier studies which focused on modelled and real urban blocks3-8. Previous study9 measured the CHTC distribution on the external surfaces of a residential district, and they examined the relationship of CHTC with the wall-adjacent wind speed. Previous study10 also measured CHTC of a window of a full-scale building by using the filter-paper evaporation method. However, field measurements are limited to measurements at specific points, it is also difficult to obtain all values of CHTC and sensible heat flux on an entire building's external surfaces with complex geometries.

Wind-tunnel experiments also have been carried out in earlier studies which focused on modified urban blocks11. Previous study12 performed wind-tunnel experiments with urban canopy models and the filter-paper evaporation method, and then measure CHTC by using the similarity between CHTC and convective mass transfer coefficient (CMTC). They then discussed the dependency of prevailing wind direction on CHTC. However, the scales of the wind-tunnel experiments are different from those of heat and mass transfer in real-building surfaces, and it is difficult to obtain similarities between CHTC and CMTC on a realistic scale. Numerical simulation is considered to be an appropriate method to understand not only the properties of flow fields around buildings, but also to determine the CHTC of entire surfaces on a consistent scale (Figure 2).

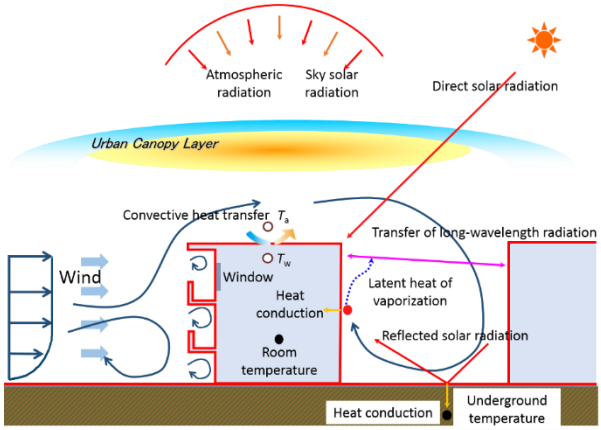

Figure 2. Diagram of sensible heat flux from external surfaces of buildings to the surrounding atmosphere.

There have been several studies which aimed to identify CHTC using numerical simulation13-16, and some turbulence models have been used. The high-Reynolds-number k–ε model (the High-Re model, where k is the turbulent kinetic energy, ε is the turbulent dissipation) is a widely used Reynolds-averaged Navier–Stokes (RANS) model which applies wall functions to cells with adjacent walls (wall-adjacent cells), so the results will not account for the behaviour inside the boundary layer, which will influence the value of CHTC. Meanwhile, CHTC can be reproduced by the wall-function in view of engineering usage in the High-Re model (Figure 3). Previous study17 used the High-Re model and predicted the CHTC of a building's external surfaces and the outdoor thermal environment in a high-rise campus block with 10-story buildings.

The Jürges equation18, shown below, is one of the most commonly used wall functions in the field of urban and built environment:

$$CHTC = 5.6 + 3.9v; \quad \text{where } v \leq 5\text{m/s}$$
$$CHTC = 7.2(v^{0.78}); \quad \text{where } v > 5\text{m/s} \tag{2}$$

where v is the wind velocity above the surface boundary layer. These equations were obtained from a single copper plate in a wind-tunnel experiment (Appendix B). Therefore, verification is necessary regardless of whether the equations are appropriate for entire building surfaces. The High-Re model has a lower computational cost and is considered to be appropriate for the prediction of sensible heat flux on the scale of an urban block in a built environment.

The low-Reynolds-number k–ε model (the Low-Re model) is another method to predict the value of CHTC, and it can also be used to simulate the wind flow and temperature fields inside the boundary layer with very fine grids. The difference between the High-Re model and the Low-Re model is a modelling level of the boundary layer. The Low-Re model is under the no-slip condition for the layer, and CHTC can be calculated by the following equation:

$$q_c = -\lambda \cdot \frac{dT}{dy} \tag{3}$$

$$CHTC = \frac{q_c}{T_s - T_{ref}} \tag{4}$$

where q_c is the sensible heat flux, W/m^2; λ is the thermal conductivity of air, W/(m·K); dT/dy is the temperature gradient inside the viscous sublayer, K/m; T_s is the surface temperature of walls, K; and T_{ref} is the air temperature above the thermal boundary layer, K.

Using the Low-Re model, the behaviour of heat and momentum transfer inside the boundary layer, which affect the value CHTC, can be reproduced (Figure 4). To ensure that at least one of the wall-adjacent cells is inside the vicious sublayer, this study examined the wall distance y^+ with value below 5 at every surface point. The wall distance y^+ is defined as

$$y^+ = \frac{u_\tau y_p}{\nu} \tag{5}$$

where U_τ is the frictional velocity, y_p is the distance from the centre point 'p' of the wall-adjacent cell to the wall, and v is the kinematic viscosity of air.

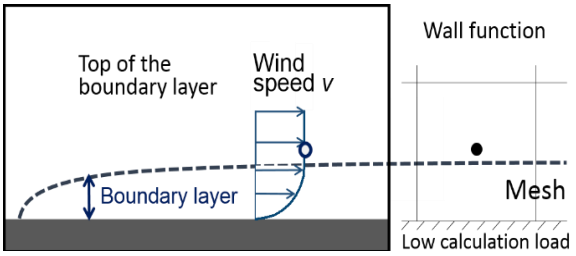

Figure 3. Wall boundary layer and the cell division near the surfaces of the Low-Re model.

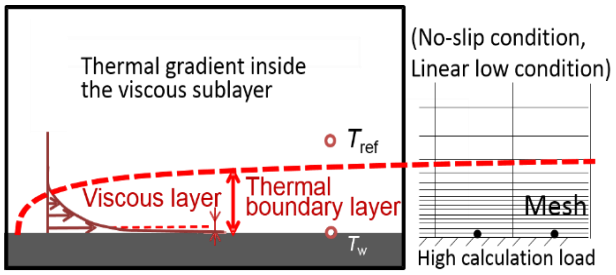

Figure 4. Wall boundary layer and the cell division near the surfaces of the High-Re model.

Since this model is based on the theory of heat-transfer, the accuracy of sensible heat flux prediction is high. Meanwhile, when the model is applied on the urban-block scale, it requires high computational cost because of the enormous number of meshes. Previous study19 used the Low-Re model to predict the CHTC distribution on the surfaces of a small building. However, the detailed geometries of the building were not reproduced, and they quantitatively analysed only the distribution of CHTC on the windward façade with a flat surface. In addition, the differences in prediction accuracy of sensible heat flux on the building external surfaces between the Low-Re model and the High-Re model have not been concretely confirmed in reality. Moreover, it is necessary to examine if it is possible to derive the CHTC-predicting equation for the High-Re model from the Low-Re model.

As suggested by the subjects mentioned above, the goal of this study was to quantitatively confirm the effectiveness of the turbulence model and spatial geometry in predict the sensible heat flux. It was further examined whether it was possible to derive a new CHTC-predicting equation that can be applied for the High-Re model from the Low-Re model. Because the forced convection field is dominant in outdoor urban spaces, except under the condition of low wind speed, in which case natural convection prevails, this study calculated CHTC under the condition of forced convection field.

2.2 Prediction of sensible heat flux

2.2.1 Target Building. This study selected one of the typical buildings located in an old residential district in Shanghai. Because this study intended to investigate the effect of surrounding flow fields for an isolated building as the first step, the surrounding buildings were not reproduced. The target building has typical geometries and is constructed of conventional materials, concrete with glass windows, for Chinese apartments. The verandas have the same pattern of arrangement and it was easy to confirm the effect of detailed geometries on CHTC. This study carried out simulations for two cases: one with detailed geometry (verandas, vertical partitions and eaves) and the other without detailed geometry.

2.2.2 Calculation Methods of Heat Balance and Coupled Analysis. This study used the 3D CAD-based thermal environment simulator to calculate surface temperature. The simulator generated cells on the external surfaces of building, and for each of the cells, this tool calculated the heat balance as follows:

$$RS + RL + QH - QE - QG = 0 \tag{6}$$

$$QH = CHTC\,(Ts - Ta) \tag{7}$$

where R_S is the net short-wave radiation, R_L is the net long-wave radiation, Q_H is the sensible heat flux, Q_E: is the latent heat flux, and Q_G is the conductive heat flux (see Chapter 5 for details).

The 3D CAD-based thermal environment simulator considers wind and temperature distribution in urban canopy as constants, so it cannot calculate the surface-temperature distribution by taking wind- and air-temperature distribution into account. To resolve the issue, this study coupled the simulator with computational fluid dynamics (CFD), which is called the coupled analysis. The flow chart of the coupled analysis is shown in Figure 5. First, this study performed isothermal air flow simulation by the CFD simulation and estimated the CHTC distribution on the entire building's surfaces. This study used the value of CHTC calculated from the forced convection field for the boundary condition of the heat-balance simulation. Then, this study performed heat balance simulation (Appendix A) and calculate the distribution of surface-temperature, taking the CHTC distribution into account. Finally, this study calculated and analysed the sensible heat flux from the CHTC and surface temperature distribution.

2.2.3 Simulation Conditions. At first, the turbulence model of the CFD simulation was used as the Low-Re model, the prediction accuracy of which is shown in Section 6.1. The High-Re model was then applied to confirm similarities and differences with the Low-Re model, and applicability to sensible heat flux prediction. Before the comparison, the relationship between wall-adjacent wind speed and CHTC is examined in the Low-Re model to derive a prediction equation which can be apply to the prediction of CHTC for the High-Re model.

Table 1 shous the simulation conditions. The cell-division section of the Low-Re model with detailed geometries is shown in Figure 6, along with an enlarged figure of the veranda. This study generated the cells near the surface with smaller size than that in the space. In terms of the cells close to the surface, this study refined it with 8 layers. This study confirmed that even at vertical partitions of the verandas, the generated cells were very fine and closely fitted to the surface. The results of wind speed obtained by the CFD simulation are shown in Figure 7. It can be confirmed that the air circulation behind the building was reproduced, and also wind speed was reduced in the veranda spaces.

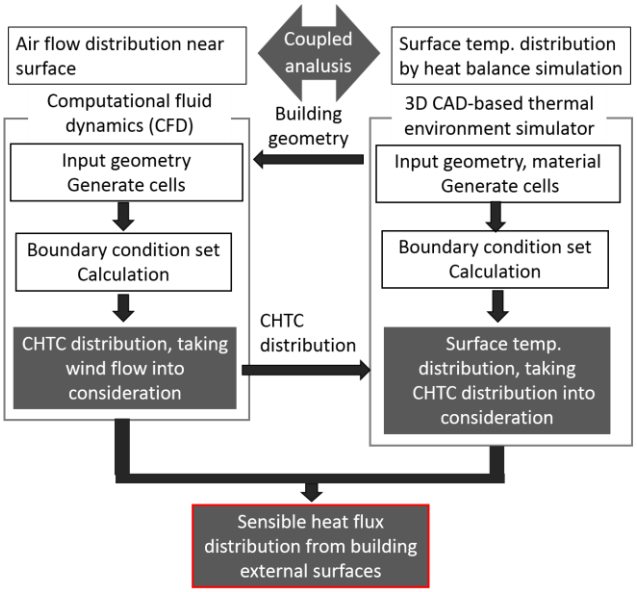

Figure 5. Flow chart of the coupled analysis.

Table 1. Simulation and weather conditions.

	Case 1	**Case 2**
Turbulence model	Low-Re number k-ε model (Lounder-Sharma model)	
Advection scheme	Upwind difference scheme	
CFD simulation tool	OpenFOAM-2.0	
Vertical profile	$v = 2.17(Z/30)^{0.2}$	
Inlet boundary	Power law	
Outlet boundary	Pressure at the interface is 0 (Pa)	
Cell numbers on building surfaces	About 4 million	About 25 million
Cell size near the surface	6.1e-5 m	
Boundary condition (ground, wall)	No-slip condition	
Calculation method of CHTC	Definition equation: $q_c = \lambda * \mathrm{d}T/\mathrm{d}y$ $\quad CHTC = \frac{\lambda \cdot \mathrm{d}T/\mathrm{d}y}{T_s - T_{ref}}$	
Weather condition	Nov. 5th 2004 12:00:00, Temp. [].2℃, Sunny, Wind speed at 1.8 times the building height: 2.0m/s, South wind	

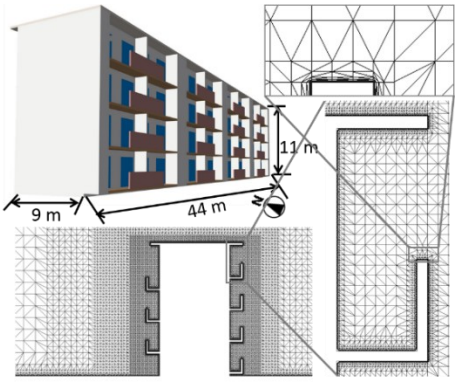

Figure 6. Simulation of the target building with detailed geometries and cell division near the surface of the Low-Re model.

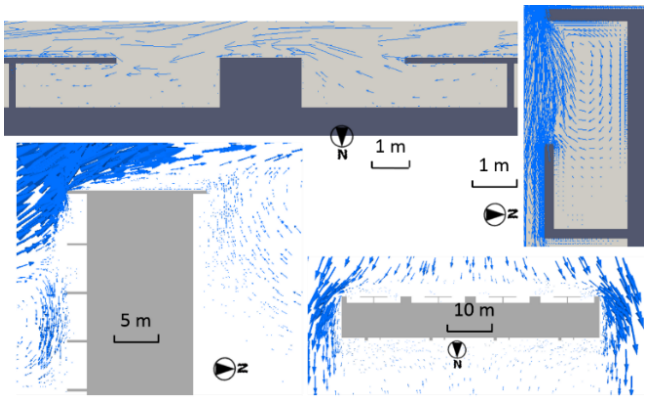

Figure 7. Distribution of wind velocity vector in the horizontal (6 m above ground level) and vertical (around the centre of the building) directions.

3. RESULTS

3.1 Effect of a building's detailed geometries on the CHTC prediction

In order to confirm the effect of detailed geometries such as verandas and eaves, which can affect the wind flow near the walls and surface temperatures, this part of study compared the case without detailed geometries (Case 1) and the case with detailed geometries (Case 2).

Figure 8 shows the distribution of CHTC on the windward facade. In both cases, CHTC distribution shows the same tendency of increasing from the bottom of the building centre to the surrounding area. Previous study19 had already reported this distribution tendency for a flat building facade. In addition, by reproducing the detailed geometries Case 2), the wind speed in the veranda space becomes small, and then CHTC of the wall becomes small owing to the obstacles in the form of eaves and vertical partitions of verandas. At the vertical partitions of verandas, there are some places on the edge where CHTC is larger than that at the centre. Case 2 shows not only the simple tendency for CHTC which increase from the bottom to the top and also increase from the centre to the sides, but also variations caused by the detailed geometries. The surface-temperature distribution in Figure 9 confirms that the surface temperature shows a tendency opposite to that of the CHTC distribution, because high CHTC takes away large convective heat transfer from the surface, decreasing the surface temperature as a result. Meanwhile, in Case 2, the surfaces of the space inside the verandas show low surface temperatures because of solar shading. As shown by the sensible heat flux in Figure 10, even though the distribution of CHTC and surface temperature caused by the air flow near the surfaces have opposite tendencies except inside the veranda space, the distributions of sensible heat flux and CHTC show almost the same trends. On the surfaces with the same solar radiation, CHTC plays a more important role than the surface temperature on the sensible heat flux. The histogram shows sensible heat flux in Figure 11. It shows that both cases exhibit similar

general trends, while the sensible heat flux of Case 1 is 20% higher than that of Case 2. Based on these findings, it shows that the detailed geometries could affect the prediction of sensible heat flux by up to 20%.

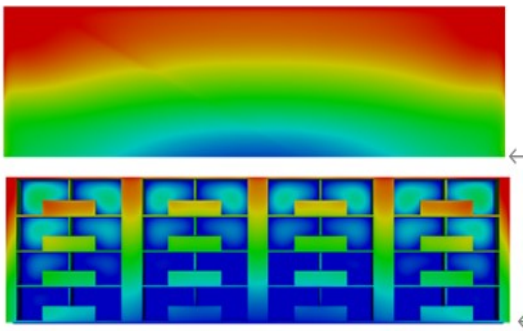

Figure 8. CHTC distribution on the windward facade of Case 1 (top) and Case 2 (bottom).

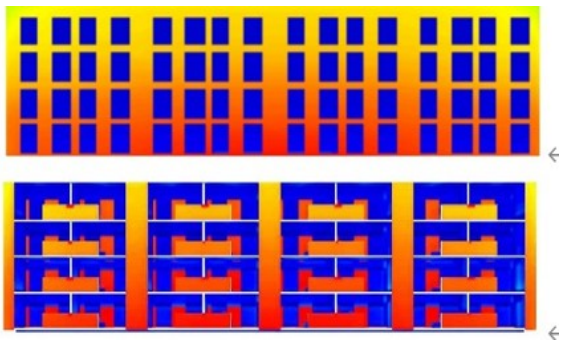

Figure 9. Surface-temperature distribution on facade the windward facade of Case 1 (top) and Case 2 (bottom).

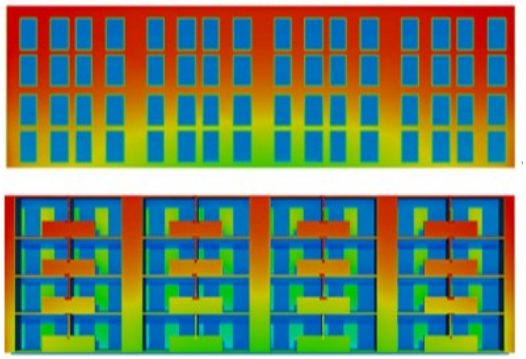

Figure 10. Sensible heat flux distribution on the windward facade of Case 1 (top) and Case 2 (bottom).

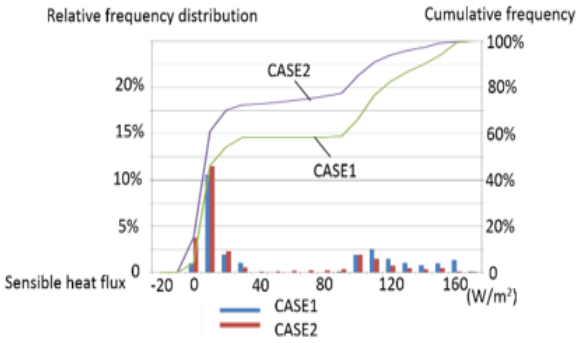

Figure 11. Histogram of sensible heat flux of Case 1 and Case 2.

3.2 Relationship between CHTC and wind speed near the surface

The relationship between CHTC and wind velocity at a distance of 10 cm above the surface U (where $U = \sqrt{U_x^2 + U_y^2 + U_z^2}$) in CASE1 is shown in Figure 12. In order to obtain higher correlations, this study added the turbulence kinetic energy k, which represents the strength of disturbance to the average wind speed to create another parameter U_k20:

$$Uk=\sqrt{U_x^2 + U_y^2 + U_z^2 + 2k} \tag{8}$$

where U_x, U_y, and and U_z are the x, y, and z component, respectively, of the wind velocity, and k is the turbulence kinetic energy.

The relationship between CHTC and U_k was also examined, and the result is shown in Figure 13. Compared to the coefficient of determination R^2 of 0.52 between U and CHTC, the R^2 between CHTC and U_k is 0.69. It shows that CHTC has a stronger correlation with U_k because in some area where the average wind speed is small but the turbulence is large, resulting in a larger CHTC. At these places, U_k is a better index than U for predicting CHTC. The correlation between CHTC and U_k for Case 2 is also shown in Figure 14. The R^2 is 0.77. In both cases, CHTC shows strong correlation to U_k for both linear and power approximation. While Case 2 shows many more values of CHTC under 4 W/(m^2·K) owing to the detailed geometries. In any case, it can be concluded that it is possible to approximately calculate CHTC using the equation of U_k.

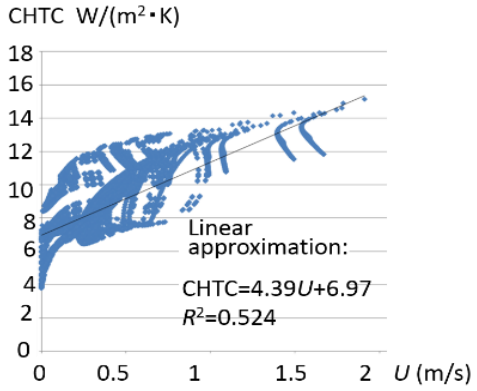

Figure 12. Relationship between CHTC and U (Case 1).

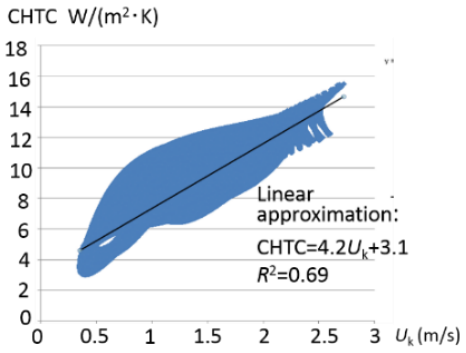

Figure 13. Relationship between CHTC and Uk (Case 1).

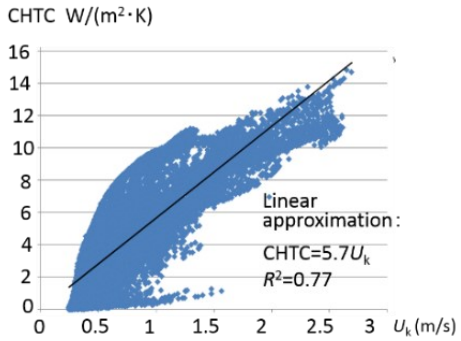

Figure 14. Relationship between CHTC and Uk (Case 2).

3.3 Difference between sensible heat flux of the High-Re model and the Low-Re model

This part of the study aims to clarify the effect of selection of the turbulence model on sensible heat flux prediction. By applying the approximation equation (called the prediction equation here) derived in the previous section to the high-Re model, it can confirm that the prediction accuracy of the prediction equation by comparing it to the Low-Re model. The prediction equation applied is CHTC = $5.7U_k$.

This study performed the coupled analysis for the High-Re model, as well as the Low-Re model, for the same target building with the detailed geometry. Hereafter, the High-Re model calculated by Jürges equation is referred to as Case 3, and the High-Re model calculated by the prediction equation is referred to as Case 4. This study compared Case 2, Case 3, and Case 4, and the results are shown in Figure 15. Overall, Case 4 shows results that are closer to those of Case 2 than Case 3. However, the edge effects on the edge of verandas cannot be confirmed from Case 4 unlike it could be confirmed in Case 2. The windward facade is divided into four areas (shown in Figure 15) and Table 2 shows the average sensible heat flux for each area, as well as the average sensible heat flux from the entire windward external surface. This study discovered that in general, for the sensible heat flux from the entire windward external surface, Case 4 also shows a result that is quantitatively closer to that of Case 2 than Case 3. Case 3 shows a -20% difference from Case 2, while Case 4 shows a lower difference of <15%. It can thus conclude that the predicting accuracy of sensible heat flux is increased by applying the prediction equation instead of the Jürges equation to the High-Re model.

The results of Case 4 still show differences from those of Case 2 (the Low-Re model). These differences originate from the modelling with wall function such as the prediction equation and the Jürges equation, and these wall functions have limitations when predicting heat and mass transfer on detailed surfaces with complex geometries. By investigating the effective wind speed U_k in the flow field of both the Low-Re model and the High-Re model, this study discovered that the average value of U_k of entire surfaces shows different values for the Low-Re model and the High-Re model. As a result, the different values of CHTC are predicted in each case. However, the surface-temperature distribution, obtained by taking into consideration the CHTC distribution, shows almost the same results. Therefore, the sensible heat flux

calculated by the prediction equation (Case 4) shows slightly different results compared with those of the Low-Re model (Case 2). Nevertheless, the prediction equation shows more reasonable values than those obtained Jürges equation in sensible-heat-flux prediction in this modelling.

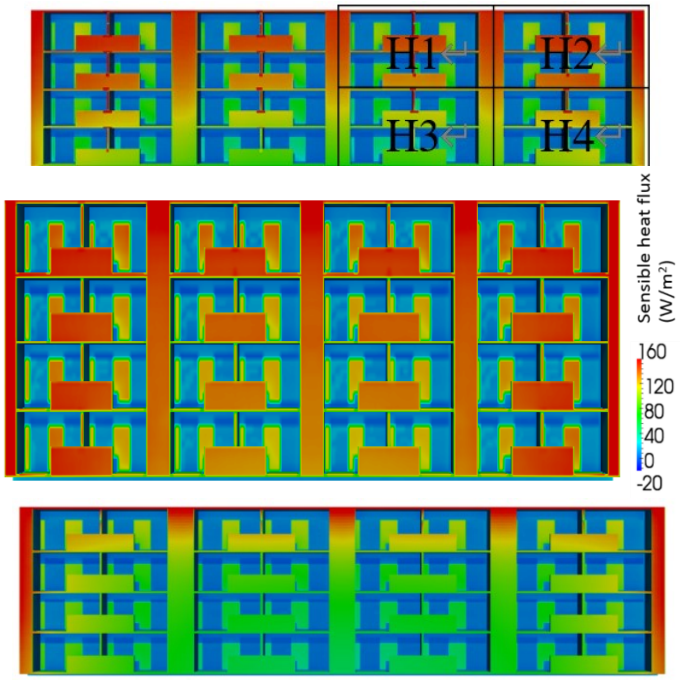

Figure 15. Distribution of sensible heat flux on the windward facade (from top to bottom for Case 2, Case 3, and Case 4).

Table 2. Average sensible heat flux from the windward façade of the building model.

		H1	H2	H3	H4	Total
Case 2	Average	42.16	44.05	23.82	28.48	35.29
	Standard deviation	54.99	57.14	36.92	41.97	49.90
Case 3	Average	44.90	46.16	36.88	40.64	42.39
	Standard deviation	53.00	55.15	47.32	52.96	52.48
Case 4	Average	37.20	40.54	18.11	27.81	31.57
	Standard deviation	47.90	51.39	24.34	38.42	43.41

4. CONCLUSION

Coupled analysis of CFD and heat balance simulation was performed to predict sensible heat flux from the building external surfaces, taking into account the surface-temperature and CHTC distributions.

This study examined the effects of a building's detailed geometries on the sensible heat flux from the building external surfaces. It can be discovered that the case with detailed geometries shows lower prediction results of sensible heat flux than that without detailed geometries. Because the surrounding wind flow fields are changed by obstacles such as verandas and by solar-radiation shielding, the wall surface temperature and the wall-adjacent wind speed inside the verandas become small. Therefore, it is important to reproduce the detailed geometries of buildings located in real urban blocks when predicting the CHTC and sensible heat flux.

This study examined both the relationship between CHTC and U and between CHTC and U_k. Since CHTC showed stronger correlation to U_k than U, this study used U_k to identify CHTC.

This study derived a prediction equation of CHTC using the effective wind speed U_k from the Low-Re model and applied the equation to the High-Re model, then compared the sensible heat flux calculated from the High-Re model with the prediction equation and that calculated by the Jürges equation to the Low-Re model. Although there are some errors in the sensible heat flux owing to the limitation of the prediction equation as the wall function, it can be found that the result calculated by the prediction equation is closer to that calculated by the Low-Re model than the Jürges equation. In this situation, it can say that the prediction equation for the High-Re model is appropriate for predicting the sensible heat flux from the external surfaces of buildings under the forced convection field. The upcoming phase of this research will also consider CHTC and sensible heat flux under mixed convection field including forced and natural convection. The model will be applied to full-scale old residential district.

ACKNOWLEDGMENTS

This work was implemented in a part of the research project entitled 'Research on the optimization design of Shanghai urban commercial public space environment in the post-epidemic era' sponsored by Shanghai Pujiang Program Fund (20PJ1419700) of Science and Technology Commission of Shanghai Municipality, China.

REFERENCES

[1] Asawa, T., Hoyano, A. and Nakaohkubo, K., "Thermal design tool for outdoor spaces based on heat balance simulation using a 3D-CAD system," Building and Environment, 43, 2112-2123(2007).
[2] Hoyano, A., Asano, K. and Kanamaru, T., "Analysis of sensible heat flux from the exterior surface of buildings using time sequential thermography," Atmospheric Environment, 33, 3941-3951(1999).
[3] Ito, N., Kimura, K. and Oka, J., "A field experiment study on the convective heat transfer coefficient on exterior surface of a building," ASHRAE Trans., 78, 184-191(1972).
[4] Sharples, S., "Full-scale measurements of convective energy losses from exterior building surfaces," Building Environment, 19, 31-39(1984).
[5] Yazdanjan, M. and Klems, J. H., "Measurement of the exterior convective film coefficient for windows in low-rise buildings," ASHRAE Trans., 100, 1087-1096(1994).
[6] Jayamaha, S. E. G., Wijeysundera, N. E. and Chou, S. K., "Measurement of the heat transfer coefficient for walls," Building and Environment, 31, 399-407(1996).
[7] Loveday, D. L. and Taki, A. H., "Convective heat transfer coefficients at a plane surface on a full-scale building façade," Int. J. Heat Mass. Transfer, 39, 1729-1742(1996).
[8] Taki, A. H. and Loveday, D. L., "Surface convective coefficients for building facades with vertical mullion-type protrusions," Proc. Instin. Mech. Engrs., 210, 165-176(1996).
[9] Hagishima, A., Narita, K., Sugawara, H. and Tanimoto, J., "Field measurement on distribution of convective heat transfer coefficient within a real-scale urban canopy," J. Environ. Eng., AIJ 73, 511-518(2008). (in Japanese)
[10] Narita, K., Nonomura, Y. and Ogata, A., "Real scale measurement of convective mass transfer coefficient at window in natural wind: Study on convective heat transfer coefficient at outside building wall in an urban area Part 1 (in Japanese)," J. Archit. Plan. Environ. Eng., AIJ 491, 49-56(1997).
[11] Barlow, J. F. and Belcher, S. E., "A wind tunnel model for quantifying fluxes in the urban boundary layer," Boundary-Layer Meteorol., 104, 131-150(2002).
[12] Narita, K., Nonomura, Y. and Ogata, A., "Wind tunnel test on convective mass transfer coefficient on urban surface: Study on convective heat transfer coefficient at outside building wall in an urban area Part 2," J. Archit. Plan. Environ. Eng., AIJ 527, 69-76(2000). (in Japanese)
[13] Awbi, H. B., "Calculation of convective heat transfer coefficients of room surfaces for natural convection," Energy and Buildings, 28, 219-227(1998).
[14] Manz, H., "Numerical simulation of heat transfer by natural convection in cavities of facade elements," Energy and Buildings, 35, 305-311(2003)
[15] Zhai, Z. and Chen, Q., "Numerical determination and treatment of convective heat transfer coefficient in the coupled building energy and CFD simulation," Building and Environment, 39, 1001-1009(2004).
[16] Defraeye, T., Blocken, B. and Carmeliet, J., "CFD analysis of convective heat transfer at the surfaces of a cube immersed in a turbulent boundary layer," International Journal of Heat and Mass Transfer, 53, 297-308(2010).

[17] Liu, J., Srebric, J. and Yu, N., "Numerical simulation of convective heat transfer coefficients at the external surfaces of building arrays immersed in a turbulent boundary layer," International Journal of Heat and Mass Transfer, 61, 209-225(2013).
[18] Jürges, W., "Der Wärmeüberergang an einer ebenen Wand (in German)," Beihefte zum Gesundheits-Ingenieur Beiheft, 19, (1924).
[19] Blocken, B., Defraeye, T., Derome, D. and Carmeliet, J., "High-resolution CFD simulations for forced convective heat transfer coefficients at the facade of a low-rise building." Building and Environment, 44, 2396-2412(2009).
[20] Hagishima, A., Tsukimatsu, K., Tanimoto, J. and Katayama, T., "Proposal of the estimation of the heat transfer coefficient on the building surfaces as the wall function of the k-ε model focuses on the outdoor thermal environment: Part 1 field measurements on both a horizontal roof surface and vertical wall surfaces of a test-house," J. Archit. Plan. Environ. Eng., AIJ 550, 23-29(2001). (in Japanese)

APPENDIX A

Heat balance calculation equations

Heat balance of each surface

$$R_S + R_L + Q_H - Q_E - Q_G = 0 \tag{A1}$$

$$R_S = a_{su}(cos\,\theta \cdot I_{DR} + F_{sky} I_{SR} + I_{RR}) \tag{A2}$$

$$R_L = F_{sky} R_{La} + R_{Lw} - \varepsilon_s \sigma {T_s}^4 = F_{sky}\left(R_{La} - \varepsilon_s \sigma {T_s}^4\right) + \left(R_{Lw} - F_w \varepsilon_s \sigma {T_s}^4\right) \tag{A3}$$

$$F_{sky} + F_w = F_{sky} + \sum_{i=1}^{n} F_i = 1 \tag{A4}$$

$$R_{La} = \varepsilon_s \sigma {T_a}^4 \left(a + b\sqrt{e}\right) \text{ (clear sky)} \tag{A5}$$

$$R_{La} = \varepsilon_s \sigma {T_a}^4 \left(a + b\sqrt{e}\right) \times (1.0 - (1-m)c/10) \quad \text{(cloudy sky)} \tag{A6}$$

$$R_{Lw} = \varepsilon_s \sum_{i=1}^{n} F_i \varepsilon_{wi} \sigma {T_{wi}}^4 \tag{A7}$$

$$Q_H = \alpha_c (T_a - T_s) \tag{A8}$$

$$Q_E = l\beta k(X_s - X_a) \tag{A9}$$

$$Q_G = -\lambda \frac{\partial T}{\partial x} \tag{A10}$$

One dimensional heat conduction (inside of each surface)

$$\frac{\partial T}{\partial t} = \frac{\lambda}{c_\rho} \frac{\partial^2 T}{\partial x^2} \tag{A11}$$

Boundary condition for indoor inside

$$-\lambda \frac{\partial T}{\partial x} = \alpha_o (T_{sr} - T_r) \tag{A12}$$

Nomenclature

R_S: net short wave radiation (W/m^2)

R_L: net long wave radiation (W/m^2)

R_{La}: atmospheric radiation (W/m^2)

R_{Lw}: long wave radiation from surrounding buildings and ground (W/m^2)

Q_H: sensible heat flux (W/m^2)

Q_E: latent heat flux (W/m^2)

Q_G: conductive heat flux (W/m^2)

T: temperature (K)

a_{su}: solar absorptivity

θ: incidence angle of direct solar radiation (rad)

I_{DR}: amount of direct solar radiation (W/m^2)

F: shape modulus (sky: sky factor)

I_{SR}: amount of sky solar radiation (W/m^2)

I_{RR}: amount of reflected solar radiation (W/m^2)

ε: long wave emittance

σ: Stefan Boltzmann constant (W/(m^{2}K^4))

a,b: constant on Brunt's formula

α_c: convective heat transfer coefficient (W/(m^2·K))

β: evaporation efficiency (-)

X: absolute humidity (kg/kg')

C_ρ: volumetric specific heat (W/(m·K))

m: coefficient of cloud altitude

T_{sr}: surface temperature for indoor side (K)

Subscripts

a: atmosphere

n: total number of objects that emit long wave radiation

e: water vapor pressure near the ground (Pa)

l: evaporation heat (J/kg)

k: mass transfer coefficient (kg/(m^{2}s(kg/kg')))

λ: heat conductivity (W/(m·K))

c: cloud amount ($0 \le c \le 10$)

α_o: over-all heat transfer coefficient (W/(m^{2}K))

T_r: room air temperature (K)

s: surface

w: surrounding buildings and ground

APPENDIX B

Validation of the CHTC prediction

In order to apply the Low-Re model to the estimation of CHTC and sensible heat flux for full-scale buildings, CFD simulations of the Low-Re model based on the RANS equations are validated in this appendix. The validation can be conducted by comparing the CFD simulation results with previous wind-tunnel experimental data or full-scale field measurements. Because the results of field measurements of full-scale buildings are generally influenced by a much larger number of factors and the measurement points are limited, wind-tunnel experimental data are considered to be more suitable for validation studies. This study will compare the CFD simulation by the Low-Re model with the wind-tunnel experiment of the two-dimensional (2D) urban canyon conducted by a previous study12.

The 2D urban canyon space is a street with buildings which have uniform height and infinite depth arranged in equal parallel intervals. This is one of the fundamental elements in the configuration of urban spaces. Previous study12 used the analogy between heat and mass transfer to identify CHTC. They applied the filter-paper evaporation method to measure the CHTC distribution of a 2D urban canyon constituted by building groups in a wind-tunnel experiment. For the validation, this study performed a CFD simulation using the Low-Re model under the same conditions (spatial form, wind speed) as those for the wind-tunnel experiment; then compared the results with the wind-tunnel experimental data of the previous study12.

Table B1. Simulation conditions.

	Turbulence model	**Meshes** **Surface cell size** **Simulation tool**	**Boundary condition**
Simulation outlines	Low Reynolds number k–ε model (Lounder–Sharma model)	About 350 thousand 1.56×10^{-6}m TSUBAME 2.0	No-slip condition

Table B1 shows the simulation conditions. The simulation model is shown in Figure B1, and simulation result is shown in Figure B2.

This study assume that the temperature and wind-speed distributions are steady after the 7th building in the 2D urban canyon model. Figure B1 shows the total façade of 7th canyon. The simulation result in Figure B2 shows a similar tendency as the result of the wind-tunnel experiment. In particular, at both ends of the canyon, it can be confirmed that there are two peaks, which is also shown by the wind-tunnel experiment. These peaks appear because near the blocks,

turbulence circulation occurs and the boundary layers of the ground at these places are undeveloped. However, at the leeward side of the block, the simulation result is slightly different from that of the wind-tunnel experiment because the circulation flow behind the building reproduced by the Low-Re model is weaker than that in reality owing to the underestimation resulting from the limitation of the k–ε model. Based on the above results, the Low-Re model shows similar results as the wind-tunnel experiment in canyon space (with a few exceptions) and can be used to estimate CHTC.

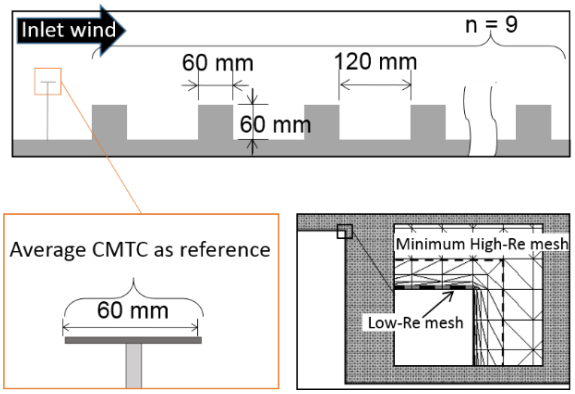

Figure B1. Simulation model for comparison with the wind-tunnel experiment.

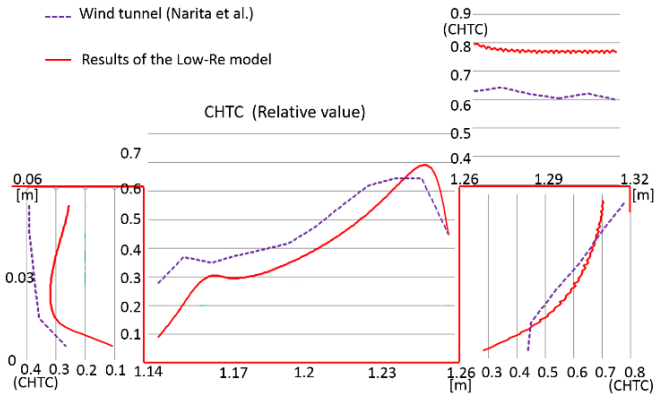

Figure B2. Comparison with the wind-tunnel experimental result for the 2D urban canyon model.